# Nitrogen deposition and climate drive plant nitrogen uptake while soil factors drive nitrogen use efficiency in terrestrial ecosystems

Helena Vallicrosa[1,2,3], Katrin Fleischer[4,5], Manuel Delgado-Baquerizo[6], Marcos Fernández-Martínez[7], Jakub Černý[8], Di Tian[9], Angeliki Kourmouli[10,11], Carolina Mayoral[11,12], Diego Grados[13], Mingzhen Lu[14,15], César Terrer[1]

**1** Department of Civil and Environmental Engineering, Massachusetts Institute of Technology, Cambridge, Massachusetts, USA.

**2** Community Ecology Unit, Swiss Federal Institute for Forest, Snow and Landscape Research WSL, CH-8903 Birmensdorf, Switzerland

**3** Plant Ecology Research Laboratory PERL, School of Architecture, Civil and Environmental Engineering ENAC, EPFL, CH-1015 Lausanne, Switzerland

**4** Department of Biogeochemical Signals, Max-Planck-Institute for Biogeochemistry, Jena, Germany.

**5** Section Systems Ecology, Amsterdam Institute for Life and Environment, Vrije Universiteit Amsterdam, The Netherlands

**6** Laboratorio de Biodiversidad y Funcionamiento Ecosistémico, Instituto de Recursos Naturales y Agrobiología de Sevilla (IRNAS), CSIC, Sevilla, Spain

**7** CREAF, E08193 Bellaterra (Cerdanyola del Vallès), Catalonia, Spain.

**8** Forestry and Game Management Research Institute, Strnady 136, Jíloviště 252 02, Czech Republic.

**9** State Key Laboratory of Efficient Production of Forest Resources, Beijing Forestry University, Beijing 100083, China

**10** Lancaster Environment Centre, Lancaster University, Lancaster, UK

**11** Birmingham Institute of Forest Research, University of Birmingham, United Kingdom

**12** School of Biosciences, Edgbaston Campus, University of Birmingham, United Kingdom

**13** Department of Agroecology, Climate and Water, Aarhus University, 8830 Tjele, Denmark

**14** Department of Environmental Studies, New York University, New York, NY 10012, USA.

**15** Santa Fe Institute, New Mexico, NM 87501, USA

Correspondence to: Helena Vallicrosa (helena.vallicrosa@gmail.com)

ABSTRACT

The role of plants in sequestering carbon is a critical component in mitigating climate change. A key aspect of this role involves plant nitrogen (N) uptake (Nup) and N use efficiency (NUE), as these factors directly influence the capacity of plants to store carbon.

49 However, the contribution of N deposition and soil factors (biotic and abiotic) in addition to
50 climate to plant N cycle, remains inadequately understood, introducing significant
51 uncertainties into climate change projections. Here, we used ground-based observations
52 across 159 field experiments (including above and belowground information) to calculate
53 Nup and NUE and identify their main drivers in natural ecosystems. We found that global
54 plant Nup is primarily driven by N deposition, mean temperature and precipitation, with
55 Nup increasing in warmer and wetter areas. In contrast, NUE is driven by soil biotic and
56 abiotic factors. Specifically, NUE decreased with the intensity of the colonization by
57 arbuscular mycorrhizal fungi and increased with soil pH and soil microbial stocks. Nup and
58 NUE presented opposite latitudinal distributions, with Nup higher on tropical latitudes and
59 NUE higher towards the poles. Total soil N stocks were not found to be a driver of Nup or
60 NUE. We also compared our results with TRENDY models and found that models may
61 overestimate Nup by ~ 100 Tg N yr$^{-1}$ in the tropics and triple the standard deviation on
62 boreal latitudes. Our findings emphasize the effect of N deposition and soil microbes that,
63 in addition to climate and soil pH, are crucial for accurately predicting ecosystems' capacity
64 to sequester carbon and mitigate climate change at a global scale.
65
66 Plain language summary
67 We used field empirical data worldwide to calculate plant nitrogen uptake (Nup) and
68 nitrogen use efficiency (NUE) in woodlands and grasslands and determine its drivers, which
69 can be used as empirical validation for models. Even though some regions of the world have
70 decreased their N deposition, N deposition is still the most important driver explaining plant
71 nitrogen uptake, aside from climatic variables.
72
73
74
75
76
77
78
79
80
81
82
83
84
85
86
87
88
89
90
91
92

## 1.Introduction

Climate and nutrient availability play significant roles in the capacity of plants to sequester carbon (C). Nitrogen uptake (Nup) and nitrogen use efficiency (NUE) are fundamental processes in plant-soil N cycling, which in turn impact biodiversity, ecosystem productivity, C sequestration, food security, and human health (Peñuelas et al., 2020). Hence, realistic quantifications of Nup and (NUE) and the understanding of their drivers are crucial to predicting the fate of terrestrial ecosystems under a changing environment. Climate, biomass production, and Nup are strongly intertwined, where hotter and wetter ecosystems have the capacity to grow more, increase their N demand, and therefore absorb more N if available (Berntson et al., 1998; Wu et al., 2011). Nonetheless, several factors can affect N availability. Traditionally, total soil N stocks were used to proxy N availability or plant Nup. Although this correlation is weak, it is still used in a modeling perspective (Stevens et al., 2015; Vicca et al., 2018) assuming that total soil N, positively correlates with N availability.

The soil community (i.e. microbes and fungi) plays a crucial role in global biogeochemical cycles governing processes such as N fixation, nitrification, denitrification and general organic matter and nutrient turnover (Aber et al., 2001; Sinsabaugh et al., 2002; Sinsabaugh et al., 2008; Crowther et al., 2019; Delgado-Baquerizo et al., 2020). In turn, the soil community can also act as a buffer in case of nutrient excess (Wall et al., 2015) or contribute to nutrient foraging in case of nutrient deficiencies (Chen et al., 2018), shaping ecosystem functioning (Bardgett and van der Putten, 2014). Therefore, the soil community is expected to substantially interfere with in the plants Nup and NUE. N deposition is another agent relevant for global N cycles, which has increased from ~30 to ~80 Tg N/year worldwide since 1850 (Kanakidou et al., 2016) with an associated increase in N availability (Elser et al., 2010; Battye et al., 2017; Peñuelas et al., 2020). Consequently, reliable quantifications of plant Nup and NUE need to include climatic factors as well as soil biotic factors and N deposition.

N regulates the capacity of ecosystems to store C (Hungate et al., 2003; Fernández-Martínez et al., 2014; 2019; Wang et al., 2017) and respond to climate change drivers (Fleischer et al., 2019; Terrer et al., 2019; Walker et al., 2021; Zhou et al., 2022) being the C-N assembly relevant for land surface models (LSM). Eight of the LSM of the TRENDY ensemble (Sitch et al., 2015), a model ensemble designed to disentangle the effects of climate, CO2, land use, and land cover change, include representations of the N cycle and plant N uptake. Nonetheless, its parameterization of N cycling is poorly constrained by observations (Zaehle et al., 2014; Fowler et al., 2015; Braghiere et al., 2022). Consequently, when models are assembled, the result leads to accumulated uncertainty (Prentice et al., 2015; Franklin et al., 2020) and therefore divergent predictions of the land sink (Zaehle et al., 2014; Stocker et al., 2016; Arora et al., 2020). Furthermore, when accounting for N interactions, LSM do generally not consider the direct effects of microorganisms' missing out on the role of soil bacteria or mycorrhizae on plant nutrient uptake. Including global calculations of plant Nup and NUE based on empirical data as well as accounting for climate, N deposition, and soil biomass interactions would potentially refine the N accountability in LSM.

137
138  Here, we gathered information from 159 plots worldwide that describe woodlands and
139  grasslands across different biomes to calculate plot-based plant Nup and plant NUE using
140  exclusively empirical field data. Our analyses combine N concentration and net primary
141  productivity (NPP) data in different aboveground and belowground plant tissues (i.e.,
142  leaves, roots, stem). We used linear models to identify the drivers of Nup and NUE, including
143  N deposition, soil microbes, woodiness, and climatic factors. We then upscaled those results
144  using the machine-learning models to quantify yearly plant Nup and plant NUE at a global
145  scale in natural terrestrial ecosystems (woodlands and grasslands) and compared these
146  results with simulations from LSM. We hypothesize that factors such as N deposition and
147  soil microorganisms have significant impacts on Nup and NUE respectively, playing a role as
148  important as climatic drivers. We expect the ground-based data, and incorporation of these
149  N-relevant drivers to increase the accuracy of global Nup quantifications. Thus, a mismatch
150  between our estimation and current TRENDY simulation outputs is expected.
151
152  **2. Results and discussion**
153  **2.1 Nitrogen uptake and nitrogen use efficiency**
154  Our findings indicate that N deposition and climate are fundamental factors explaining plant
155  Nup on a global scale (Fig. 1). Further analysis revealed a positive relationship between Nup
156  and accumulated N deposition, mean annual temperature (MAT), and mean annual
157  precipitation (MAP). Thus, regions that are warm, wet, and with higher levels of N
158  deposition, exhibit the highest rates of Nup. Our results show that N deposition is strongly
159  contributing to fulfilling the N demand in productive environments, alleviating potential N
160  limitations and allowing high plant Nup levels. On the other hand, our empirical results did
161  not show important relationships between plant Nup and soil microbial interactions nor soil
162  physico-chemical variables (Fig. 1a). Those results include no significant relationship
163  between soil N stocks and Nup at a global scale (Fig. S1a), which has been further tested
164  following a univariate approach. This result discourages the use of soil N to infer N
165  availability.

**Plant nitrogen uptake**
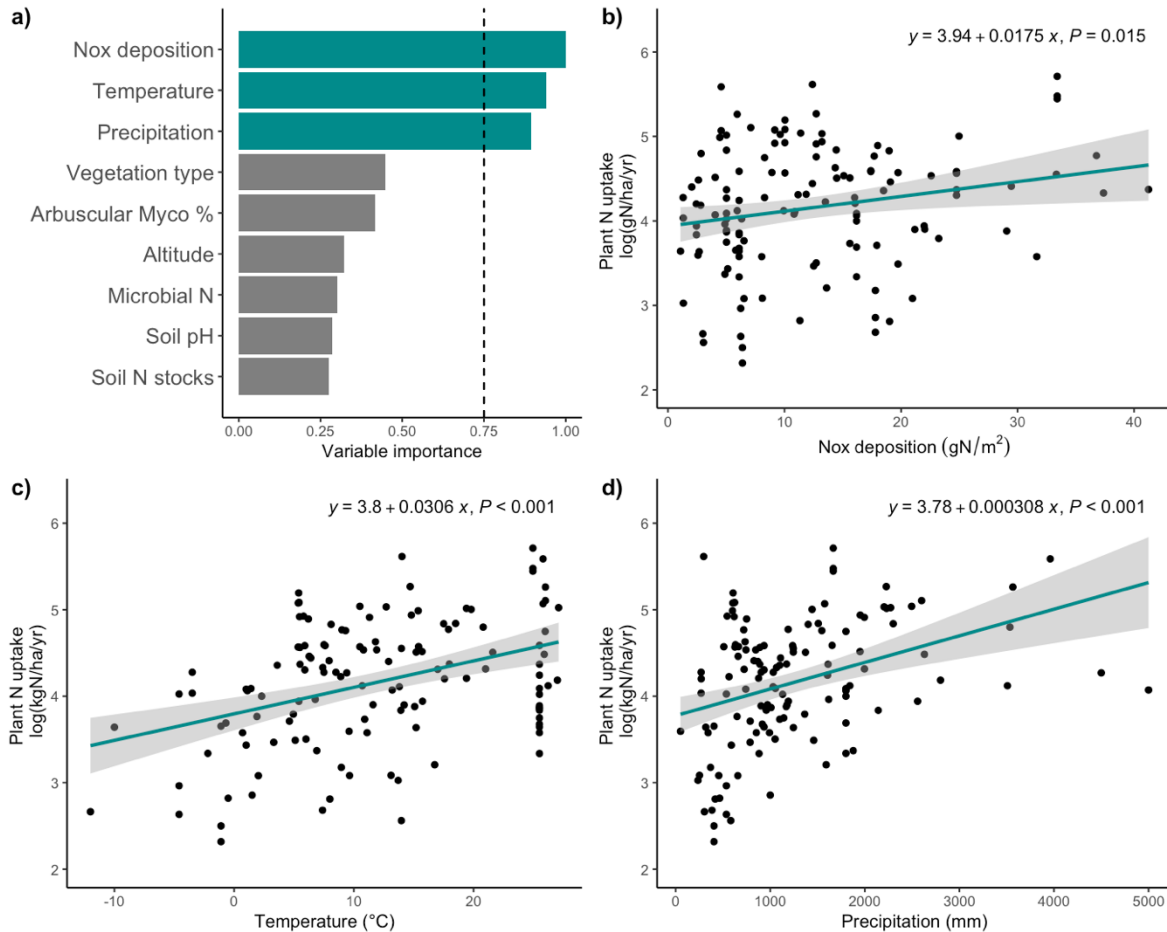
166
167 *Figure 1. a) Variable importance plot for the general linear model (GLM) describing plant nitrogen uptake (Nup). The*
168 *dashed line is set at 0.75, separating the threshold for important variables. The GLM model pseudoR$^2$ was 0.349. Linear*
169 *regressions were displayed describing plants' nitrogen and important variables b) accumulated Nox deposition from 1901*
170 *to 2021, c) mean annual temperature, and d) mean annual precipitation. Equation and p-value per regression displayed.*
171 *Acronyms: Nox: oxidized nitrogen, N: nitrogen, Myco %: Mycorryzal percentage.*

172  In contrast, when describing NUE, our model selection analysis identified soil biotic and
173  abiotic factors as the main NUE drivers (Fig. 2). Specifically, our results described NUE
174  decreased with AM % but a positive relation between soil pH, soil microbial N stocks and
175  NUE was found. Thus, plant species prone to be colonized by arbuscular mycorrhizae, are
176  less efficient in N use to build biomass. In contrast, basic pH and abundant soil microbial
177  stocks facilitate higher NUE rates. Even though soil variables appear to be important for
178  NUE, soil N stocks remain unrelated to NUE in the model and when tested individually (Fig.
179  S1b). Despite climatic variables such as MAT and MAP not appearing as important variables
180  explaining NUE, they are to some extent represented in the soil variables. As shown in Table
181  S2, soil variables are not independent of climatic variables since they have some degree of
182  correlation.
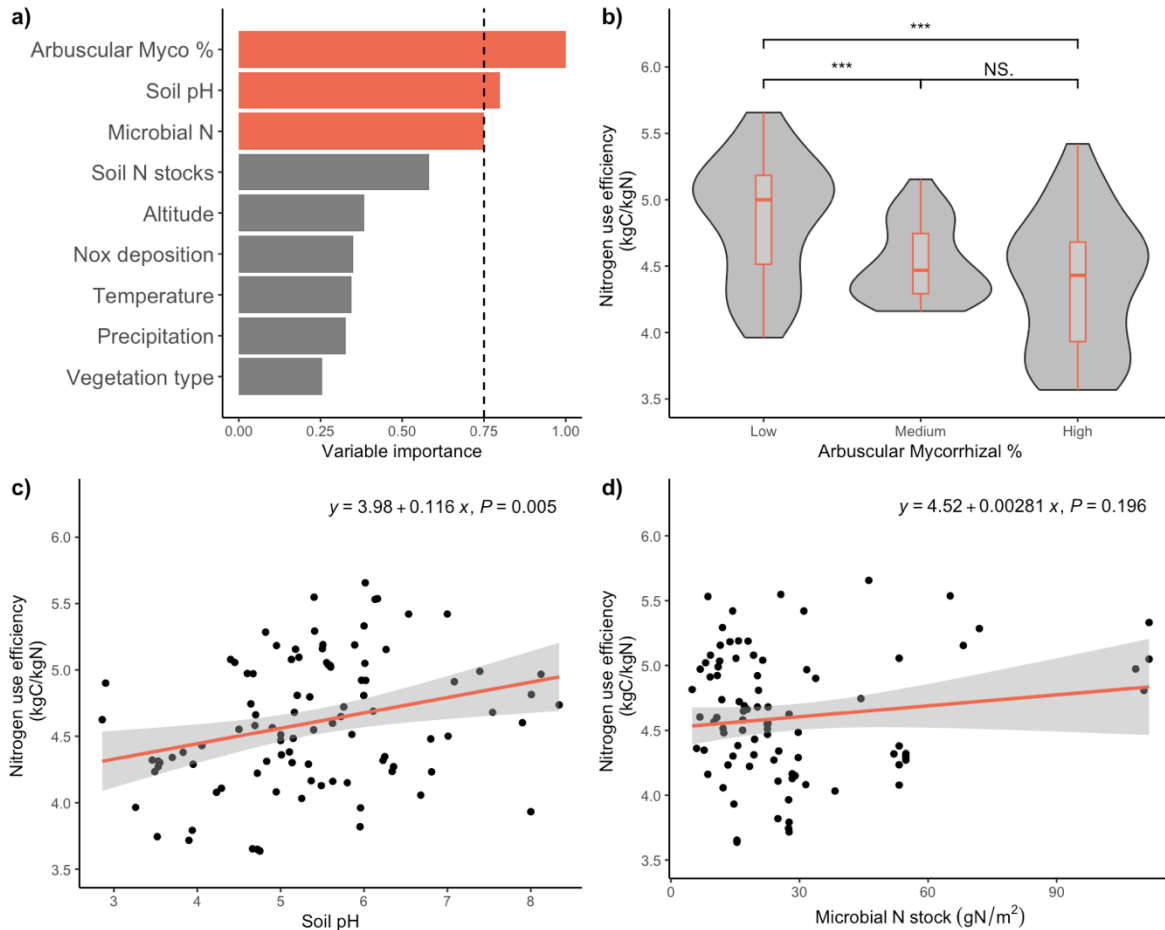
*Figure 2. a) Variable importance plot for the generalized linear model describing nitrogen use efficiency (NUE). The model preudoR2 was 0.355. The dashed line is set at 0.75, separating the threshold for important variables. In b) arbuscular mycorrhizae percentage is divided into low, medium, and high, and NUE is displayed. \* = P-value < 0.05, \*\* = P-value < 0.01, \*\*\* = P-value < 0.001. Linear regressions were displayed describing plants' nitrogen use efficiency c) soil pH and d) microbial N stocks. Equation and p-value per regression displayed.*

## 2.2 Global maps of Nup and NUE

Next, we used a machine-learning model to understand the global magnitude and distribution of Nup and NUE when the relationships found at the site level are extrapolated at a global scale. For methodological consistency, the XGBoost model was trained using the same nine variables as the linear model. We identified temperature, precipitation, and N deposition as the most critical factors for describing Nup (Fig. S2), which aligned with those in the linear model, albeit in a slightly different order. Partial dependence plots further corroborated these relationships, showing consistent correlation signs with those observed in the linear models (Fig. S3). The upscaled Nup map showed a total yearly Nup of 842.215 ± 236.11 Tg of N, with a mean coefficient of variation of 26.77 % (Fig. S4) and an $r^2$ of 0.54 (Fig. S2). The lowest Nup values were on boreal latitudes and mountain ranges such as the Rocky Mountains in the USA, the Andes in South America, the different mountain ridges in Europe, and the Himalayan plateau in Asia. The higher rates of Nup are predicted in temperate latitudes in Europe, the eastern United States, Southeast Asia, East Australia,

203 most of South America, and central Africa, with the most intense spot around Congo, where
204 there is the most N deposition, temperature and precipitation combined (Fig. 3a).
205 Therefore, Nup map shows an NPP influence, driven by temperature and precipitation, but
206 added to an N deposition distribution that shades the strictly latitudinal distribution of Nup.
207
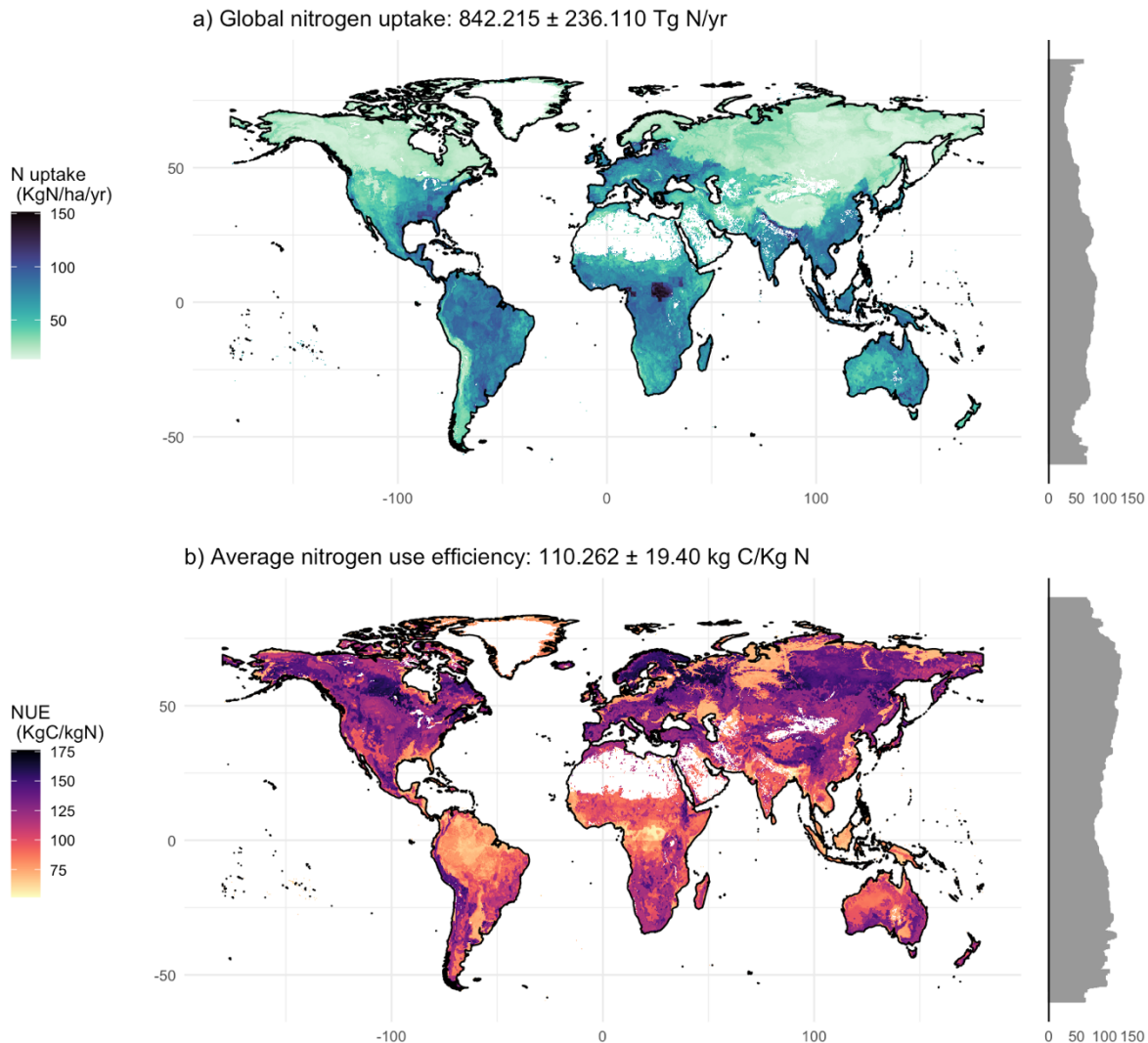
208
209 *Figure 3. Upscaled global maps describing a) Plant nitrogen uptake and b) Nitrogen use efficiency. The total amount of*
210 *nitrogen uptake calculated per year is 842.215 Tg of N with a standard deviation of ± 236.11. The mean value of global*
211 *nitrogen use efficiency is 110.26 kg of C per kg of N, and its standard deviation is 19.40. White color describes no data due*
212 *to a lack of grasslands or woody vegetation.*

213 The machine-learning models describing NUE showed the importance of microbial N stocks,
214 altitude, precipitation, soil pH, and AM% as NUE drivers (Fig. S5). These results generally
215 align with the variable importance shown in the linear models, with the addition of
216 precipitation and altitude. The variables´ relation showed similar general trends as in the
217 linear model (Fig. S6). The average predictions for NUE at a global scale were 110.262 units
218 of C per unit of N with a mean coefficient of variation of 17.89 % (Fig. S4) and an $r^2$ of 0.44
219 (Fig. S5). The map distribution showed general lower NUE around the Equator, and

220 progressively increasing towards the poles. Nonetheless, some heterogeneous parches
221 alternating high and low NUE can be found between 50 and 60 degrees latitude north (Fig.
222 3b).
223
224 **2.3 Global-scale Nup comparison with TRENDY models**
225 We further seek to compare our estimates for the total yearly Nup upscaled from field
226 observations with the mean of the Nup provided by the eight models included in TRENDY.
227 When comparing TRENDY Nup with our Nup upscaled projections, we found clear
228 geospatial pattern differences. TRENDY models produce higher Nup in the tropical regions,
229 reaching differences of around 100 kg N ha$^{-1}$ yr$^{-1}$ in those areas (Fig. 4a) representing more
230 than 100% of the Nup estimated by field observations (Fig. 4b). Other areas like the north
231 and northeast of North America, Southeast Asia, and north of Eurasia also appear to have
232 higher Nup values in TRENDY models than in field observations. In boreal latitudes, the
233 TRENDY models deviation for Nup could even reach 300% of overestimation. On the other
234 hand, areas where the upscaled approach projects higher values than the TRENDY models,
235 are the austral latitudes, the Middle Eastern regions, the Somali peninsula, and the Rocky
236 Mountains (Fig. 4). Overall, TRENDY models estimate higher values of Nup, by 16.61 kg N
237 ha$^{-1}$ yr$^{-1}$, meaning the 48.54 % of the variability. When aggregating the total year Nup, LPX-
238 Bern and CLM5.0 were the models that predicted overall values exceeding our range of
239 confidence, assuming a significantly larger Nup (Fig. S7).
240
241
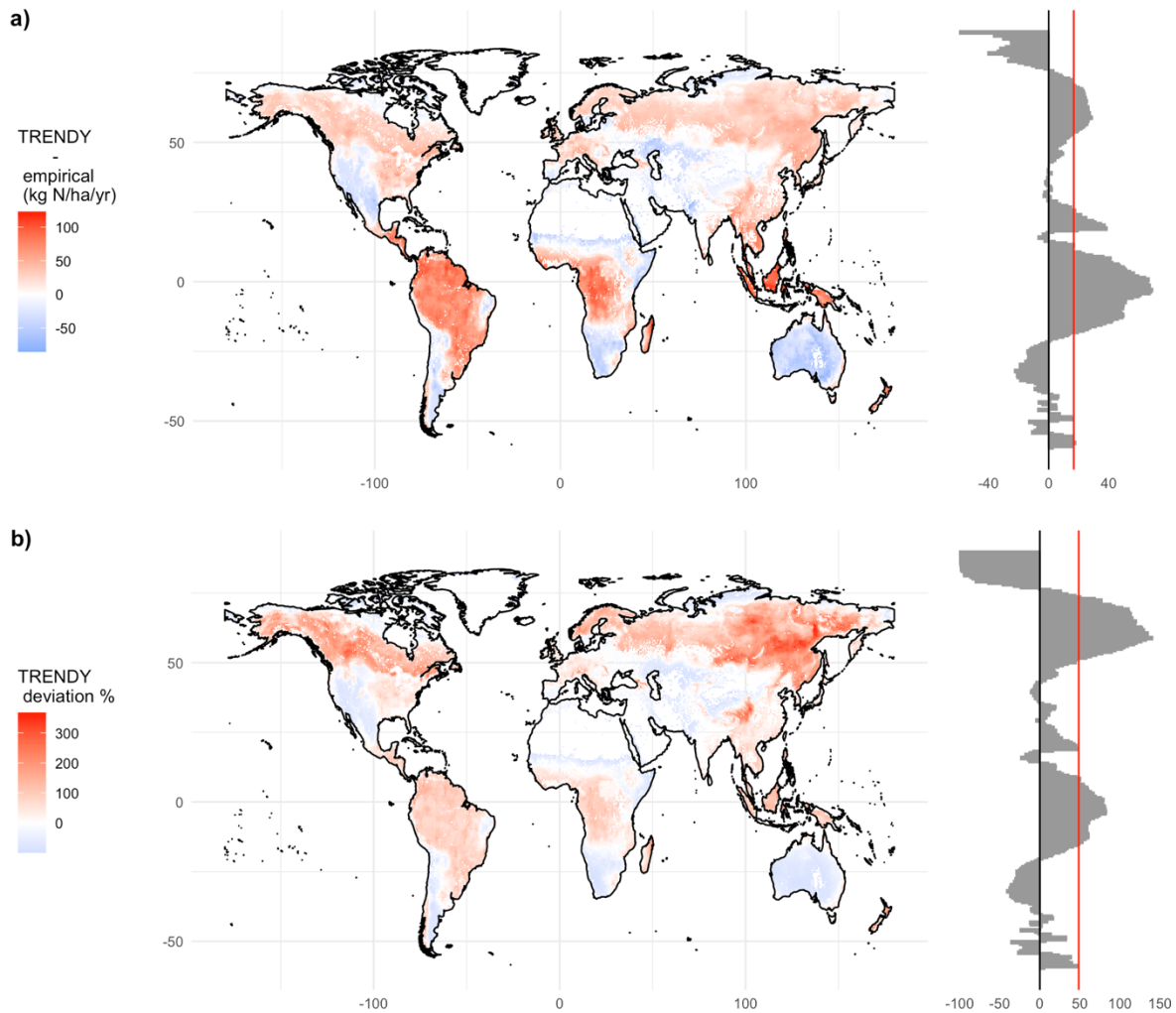
*Figure 4. Comparison between the mean of the nitrogen uptake provided by TRENDY v8 models minus the upscaled nitrogen uptake. The red color stands for higher values on the TRENDY model, and the blue color stands for higher nitrogen uptake values on the upscaled approach. In a) units in kg N ha$^{-1}$ yr$^{-1}$ and in b) units in percentage of deviation from field upscaling. Latitudinal aggregation on the right, with a red vertical line showing a ) the mean of the total comparison at 16.61 kg N ha$^{-1}$ yr-1 and b) the mean percentage of deviation at 48.54%.*

## 2.4 Nup global drivers and implications

Our models estimated the annual global plant Nup at 842 ± 236 Tg of N. This figure is consistent with the findings of Peng et al., 2023, which estimated 950 ± 260 Tg of N, and Braghiere et al., 2022, with an estimated uptake of 841.8 Tg N. The slight variations can be attributed to differences in methodologies and data sources (simultaneous plot-averaged records vs individual-level records) used in these studies. In our study, linear models and machine learning models are consistent when determining N deposition, temperature, and precipitation as global drivers of Nup. Hotter and wetter environments increase biological activity, leading to more biomass production and therefore more N demand. An increase in N demand with enough N availability is associated with an increase in Nup. The accumulation of N deposition throughout time originating from anthropogenic sources has been increasing the N availability in some areas, generally close to industrial or agroforestry pools. Hence, in a global change context where $CO_2$ fertilization and temperature increase

261     have generated a greening effect (Ruehr et al., 2023), areas with higher N deposition were
262     able to better supply the increasing N demand. Thus, according to our results,
263     anthropogenic N supply may have become a Nup driver as important as climate.
264
265     These results are concerning since our data emphasize the far-reaching influence of human-
266     induced nitrogen deposition in shaping global Nup patterns. Some regions such as Europe,
267     the Eastern USA, and the tropics have decreased their N deposition levels during the last
268     four decades (Ackerman et al., 2019). Nonetheless, these reductions do not translate yet
269     into how N deposition effects natural woodlands and grasslands, showing to still be the
270     main driver for plant Nup. This sustained entrance of anthropogenic N has been associated
271     with a fertilization effect, enhancing the land C sink by 0.72 Pg C yr$^{-1}$ during the 2010s
272     (Gurmesa et al., 2022). Nonetheless, this N fertilization effect showed evidence of
273     saturation in forests and grasslands (Tian et al., 2016; Peng et al., 2020), where the biomass
274     production and therefore the C sink increase slowed down. Consequently, this extra input
275     of N coming from N deposition is not being captured by biomass and enhances the N
276     leaching associated with eutrophication, acidification, loss of biodiversity, and $N_2O$
277     emissions (Aber et al., 1989; Gundersen et al., 1998; Bobbink et al., 2010) exacerbating
278     environmental problems.
279

280     **2.5 NUE global drivers and implications**
281     Our results predict a mean NUE of 110 ± 19 kg C per kg N. Our results indicate soil biotic and
282     abiotic factors drive NUE in natural ecosystems. The main divergence between linear
283     models and machine learning models is the importance of altitude and precipitation, which
284     showed explicit relevancy only in machine learning models. We attribute these differences
285     to the nature of the models, where machine-learning models accommodate correlations
286     without modifying their variable importance. Thus, the important variables in the linear
287     model could also have embedded important latitudinal gradients and therefore altitudinal
288     or precipitation gradients. Our NUE predictions contrasted with Peng et al., 2023, which
289     predicts a mean NUE of 76 ± 26 kg C per kg of N. The main difference between studies is
290     that our approach included biotic factors, such as mycorrhizal associations and microbial
291     interactions, that described NUE better than abiotic factors. In contrast, Peng et al., 2023
292     focused their predictions only on abiotic factors. In that regard, we do not consider
293     environmental variables such as precipitation to be totally detached from NUE relations,
294     since they are somewhat drivers of important biotic variables such as AM %, soil pH, and
295     microbial N stocks. Nonetheless, the results showed that including biotic variables may
296     result in more efficient use of N by plants at a global scale.
297

298     The response of NUE has been postulated as a method to assess N saturation in plant
299     communities (Shcherbak et al., 2014). A negative relation between N addition and NUE and
300     lower NUE levels would indicate N saturation (Iversen et al., 2010). In our study, tropical
301     areas are shown to have the lowest NUE, being the less N limited and matching with
302     previous global upscaling studies using different approaches (Du et al., 2020; Vallicrosa et
303     al., 2022). According to the soil age hypothesis (Walker and Syers, 1976), N accumulates in
304     ecosystems through time due to biological processes. Thus, newer formation areas, such as

high elevation or lower pH areas are those showing higher values of NUE and where N is expected to be more limiting. Our results only show a modest effect of N saturation due to N deposition, so further studies are needed to better assess where and under what circumstances areas are N saturated due to N deposition.

Biological activity, such as the type of mycorrhizal associations and soil microbes N stocks, was found to have a strong impact on the terrestrial N cycle. Arbuscular mycorrhizal associations are the most abundant in the tropics (Soudzilovskaia et al., 2019) and are theorized to be more efficient in nutrient capture and more abundant in areas with fast N cycling (Averill et al., 2019). Our models show that AM associations have lower NUE, possibly driven by the abundance of N and the high efficiency of AM associations in N acquisition. Conversely, N obtention was more efficient in areas with high soil microbes stocks. As described by Kuzyakov and Xu 2013, we hypothesize a potential competition effect between soil microbes and plants for N, but further studies are needed to corroborate this relation. Thus, given the importance of biological activity in fixing and transforming N, it is reasonable that total soil N stocks, that include N in all forms and aggregations, would not be a good indicator of N availability and plant N uptake.

### 2.6 Latitudinal discrepancies between Nup map and TRENDY
LPX-Bern and CLM5.0, models included in the TRENDY ensemble, projected Nup values significantly above our estimations, being 1471 and 1454 Tg N/yr respectively (Fig. S7). Even though the average of all TRENDY models falls within our Nup confidence range differences become relevant through space. In tropical and northern latitudes, TRENDY models projected higher values than our estimations. On the other hand, TRENDY models projected lower Nup values in southern latitudes, western Asia and at the Rocky Mountains. This mismatch could be associated with an overestimation of terrestrial C sink capacity and a misinterpretation of the role of vegetation in N cycling. A possible explanation of this phenomenon would be the overestimation of biomass production by LSM when not accounting for growth-limiting factors such as phosphorus availability, drought, or overall biotic competition. Alternatively, overestimation when accounting for N concentration in tissues could also lead to Nup overestimation, which would necessarily reflect in overall lower NUE values. In our calculations, we embraced the variability of N concentration and net primary productivity among tissues and leaf resorption to generate more accurate Nup and NUE values.

### 2.7 Representativity and future research
An inherent challenge in ecological studies of this scale is to ensure the global representativeness of the dataset since systematic geographical sampling biases are underrepresenting the global south. In this study, 28 % of the data comes from areas below 15º latitude, outside the US, Europe, or China (Fig. S8). When accounting for ecosystem representativity, the Whittaker diagram shows we have a representation of all the biomes (Fig. S9), showing the lowest representativity on subtropical deserts, tundra, and temperate rainforest. Nonetheless, we acknowledge that calculations based on empirical data, especially when a portion of the data has undergone a gap-filling process, can still have

349  biases associated with sampling and the upscaling process, which are mainly defined by the
350  more represented biomes of the observations. Still, we believe that calibrating and cross-
351  checking models built over mathematical assumptions with field measurements is
352  necessary to better root models to reality.
353
354  Global scale approaches such as this one, are intended to provide broad quantifications of
355  planetary processes assuming a scale-precision compromise. Because of that, we do not
356  advise using our approach to seek fine-scale precision, since our results may overlook local
357  particularities and differences between forest type, species distribution, or management
358  practices.
359
360  This study is focused on a quantitative approach at a global scale, attempting to target
361  variables' relative importance on Nup and NUE along with its correlations to environmental
362  and biotic variables. In future research, specific data detailing the different N fractions
363  obtained at a global scale (e.g. organic-inorganic, ammonium-nitrate) and a more
364  mechanistic frame are strongly encouraged. We also encourage empirical studies sampling
365  underrepresented biomes, specially from the global south. Approaches such as those in Niu
366  et al., 2016 quantifying the fraction of Nup taken by plants, leached and retained in the soil
367  at a global scale are crucial to enhancing our understanding of the N cycle and its
368  interactions with ecosystems.
369
370  **3. Conclusion**
371  We showed that accumulated N deposition and climatic variables are the main global-scale
372  factor describing Nup, where regions that are warm and wet and also experience higher
373  levels of N deposition, exhibit the highest rates of Nup. This result highlights the far-
374  reaching influence of nitrogen deposition in shaping the global Nup pattern. Interestingly,
375  NUE was shown to be driven by soil biotic and abiotic factors, emphasizing the importance
376  of soil microorganisms and pH as regulators of the N cycle. We further revealed that total
377  soil N stocks are not a Nup nor NUE driver. Our upscaling showed large spatial-explicit
378  differences with TRENDY Nup values, where TRENDY projects higher absolute values around
379  the tropics and higher deviation values in boreal latitudes. This mismatch in the spatial
380  correlation between empirical data and land system models could substantially affect
381  model accuracy and future predictions of the C sink, where the tropical capacity to store C
382  might have been overestimated. Our results provide insights to understand better the C –
383  N interactions, N cycling, and absorption in terrestrial ecosystems and highlight that N
384  deposition largely impacts plant Nup worldwide.
385
386  **4. Methods**
387  **4.1 Data extraction**
388  We gathered 159 field plot data representing 129 different sites in natural conditions
389  coming from published data or repositories (Table S1). The data included information on
390  the dominant species and vegetation type (grassland, coniferous, or broadleaved), foliar
391  and root N concentration, foliar and root biomass production, and stem biomass production
392  in the case of woody plants at the same location and time. In situ measurements for foliage

393    and fine roots are the most relevant for Nup calculation (Dybzinski et al., 2024), so all our
394    data points include biomass production (NPP) and N content (N%) of leaves and roots. We
395    gathered 45 data points, representing 28% of the data, coming from latitudes under the 15º
396    latitude, despite the systematic lack of field sampling on some regions of the earth such as
397    the global south. We also complemented the dataset with field values of litter biomass
398    production, litter N concentration, stem N concentration, soil pH, soil C %, soil N %, soil
399    texture, soil moisture, mean annual precipitation, mean annual air temperature, and
400    altitude. We included woody and grassland natural environments (Fig. S8), including
401    representation from most biomes according to Whitakker's diagram (Fig. S9). Each data
402    point covered by the analysis has been collected from 1984 to 2022. If stem N was missing,
403    happening in 25% of the data entries, we gap-filled it with the mean value of its vegetation
404    type (coniferous=0.33 or broadleaved=0.52%). With leaves, stem and roots we calculated
405    the gross Nup (see in the next section). By subtracting the amount of N recovered during
406    leaf senescence we obtain the net Nup. If litter biomass was missing, 52% of the time, we
407    assumed it to be the same amount of green leaf biomass production. If litter N
408    concentration was missing, we calculated the net Nup using the predicted value from a
409    linear model created with net Nup in the base of gross Nup, in 33% of the entries. This
410    model had an r2 of 0.88, a p-value < 2.2e-16, and a correlation of 0.72 between gross and
411    net Nup.
412
413    We extracted mean annual precipitation from WorldClim2 (Fick and Hijmans, 2017), as well
414    as soil pH, soil C, and soil N, soil moisture, soil bulk density, and soil texture from soilGrids
415    (Poggio et al., 2021). All soil data for the topsoil layer (0-15 cm). We also identified the
416    potential mycorrhizal association from the dominant species (% of colonization) based on
417    Soudzilovskaia et al. 2020, and categorized it into 0, 50, or 100 arbuscular mycorrhizal (AM)
418    percentages, since AM is the most abundant and common throughout the globe. When
419    dominant species were not provided, we extracted the AM% of colonization based on the
420    AM map of Soudzilovskaia et al. 2019 and the coordinates of our samples. Moreover, we
421    extracted the microbial N stock from Xu et al. 2013. We calculated and obtained the
422    accumulated oxidized N deposition from Yang and Tian, 2022 from 1901 to 2022 by
423    georeferencing each field plot. Oxidized and reduced N deposition are correlated and are
424    thought to have similar ecological effects (Sutton and Fowler, 1993; Yang and Tian, 2022).
425    Oxidized forms generally come from combustion reactions while reduced forms generally
426    come from agricultural practices. We decided to use the oxidized form because it is the
427    most equally distributed at a global scale.
428
429    **4.2 Nitrogen uptake and Nitrogen use efficiency calculation**
430    We calculated the increase in annual N stock for each tissue (leaves, stem, roots, and litter)
431    by multiplying the biomass increase by its N concentration. We obtained the gross annual
432    Nup by aggregating tissue's Nup (roots, leaves, and stem if woody). To account for the N
433    that has been reabsorbed before senescence, we subtracted the litter N stock from the
434    green leaves N stock. We subtracted the reabsorbed N from the gross Nup to obtain the
435    final net Nup value as follows:
436

$$Nup = (NPPleaves * Nleaves + NPPstem * Nstem + NPProots$$
$$* Nroots) - (NPPleaves * Nleaves - NPPlitter * Nlitter)$$

*Nup* = Plant nitrogen uptake (kg N/ha/yr)
*NPP* = Net primary production (kg of biomass/ha/yr)
*N* = Nitrogen (% in dry weight)

We calculated the nitrogen use efficiency (NUE) by calculating the total amount of biomass produced in leaves, stems, and root tissue divided by the amount of nitrogen in each tissue. It will give the amount of biomass produced by a unit of nitrogen.

$$NUE = (NPP_{leaves} / Nup_{leaves}) + (NPP_{stem} / Nup_{stem}) + (NPP_{roots} / Nup_{roots})$$

*NUE* = Nitrogen use efficiency (kg C / kg N)
*NPP* = Net primary production (kg of biomass/ha/yr)
Nup = Plant nitrogen uptake (kg N/ha/yr)

## 4.3 Linear statistical analysis

Nup and NUE values correlate 34% (Fig. S10). From the available variables collected, we selected the less correlated ones using the *cor* function in R to deal with multicollinearity. The less correlated variables selected were mean annual air temperature, mean annual precipitation, altitude, arbuscular mycorrhizae percentage, microbial N stock, soil N stock, soil pH, accumulated oxidized N deposition from 1901 to 2022, and woodiness. The biggest collinearity among variables was 0.52 between mean annual temperature and AM presence (Table S2). With the less correlated variables, we created generalized linear models using Nup and NUE as dependent variables. The family was set up as Gamma with an inverse link to fulfill the residual normality requirements. We also calculated the Variance Inflation Factor (VIF) with the *vif* function of the car R package (Fox and Weisberg, 2019) of the aggregated model to validate VIF's lower than 4. We performed a model selection using the *dredge* function in the MuMIn R package (Barton, 2023) and chose the best linear model based on its lowest AIC. We calculated the variable importance using the function *sw* on the MuMIN R package (Barton, 2023), which is a standard method based on Akaike weights (Giam and Olden, 2016). We calculated the pseudo R square of the models using the function pR2 from the package pscl (Jackman, 2020). Figures were created using the R package *ggplot2 (*Wickham, 2016*)*.

## 4.4 Nitrogen uptake and nitrogen use efficiency upscaling

To upscale Nup and NUE to global grasslands and woody vegetation, we used extreme gradient boosting (XGBoost) models splitting the database into train, test, and validation using a standard ratio of 70:20:10, respectively (Lever et al., 2016). Extreme gradient boosting is a machine learning algorithm that builds ensemble decision trees, applying regularization and pruning techniques to improve performance and prevent overfitting (Chen et al., 2016). XGBoost is a non-parametric model particularly indicated for high performance in sample sizes above 100 data points, overcoming potential problems of autocorrelation and optimizing predictive power. We trained an XGBoost model using the

482    R package *xgboost* (Chen et al., 2023), forcing an early stop based on minimum root mean
483    squared error to avoid overfitting and setting up the objective as a gamma regression. We
484    optimized the parameters based on performance (prediction $R^2$) at a maximum depth of 6,
485    minimum child weight of 1, and eta of 0.3, which are generally standard values. We
486    considered the same independent variables included in the linear model without
487    interactions. We repeated this process 20 times with random database separation to
488    stabilize the variability due to randomness in subset splitting. We extracted the variable
489    importance of each model using the function *xgb.plot.importance* on the *xgboost* R package
490    (Chen et al., 2023), calculated the mean of the values among the 20 different training sets,
491    and displayed it using ggplot. We calculated partial dependence plots using the function
492    *partial* in *purrr* R package (Wickham and Henry, 2023) to explore the non-linear relations
493    on the models. To calculate the model performance, we calculated the mean squared error
494    of the test set and the r squared of the predicted vs observed in the validation subset,
495    considering the validation set as completely independent.
496
497    To predict the values at a global scale, we used the spatial explicit mean annual
498    precipitation, mean annual temperature, and altitude variables provided by WorldClim2
499    (Fick and Hijmans, 2017); the microbial N stocks by Xu et al. 2013; the oxidized accumulated
500    N deposition from 1909 to 2022 calculated from Yang and Tian 2022 and soil N stocks and
501    soil pH provided by soilGrids 2.0 (Poggio et al., 2021) at 15 cm depth. We reclassified the
502    European Space Agency Land Cover (ESA-LC) map (Defourny, 2019) (Table S3) and we
503    downscaled its resolution to 2 km using the raster R package (Hijmans, 2023). We upscaled
504    each of the 20 Nup and NUE models using the trained XGBoost models and their prediction
505    per pixel at 2 km resolution and calculated the mean to obtain the final maps. We
506    parallelized the process using the *parallel* function and *spaDES.tools* R package (McIntire
507    and Chubaty 2023) to accelerate the upscaling. We masked areas not considered woodlands
508    or grasslands in natural conditions according to the European Space Agency cover map
509    (Defourny, 2019) (Table S3), and then, we obtained a map of the yearly Nup, Nup standard
510    deviation, and annual NUE. We obtained the final number of yearly Nup by summing all the
511    pixels available.
512
513    **4.5 Nitrogen uptake comparison with TRENDY models ensemble**
514    We obtained the available Nitrogen uptake of Vegetation (fNup) variable associated with
515    all the available models in TRENDY v8 S3 (Sitch et al., 2015; Le Quéré et al., 2018). The
516    models containing fNup are ORCHIDEE, LPX-Bern, LPJ-GUESS, JULES, JSBACH, DLEM,
517    CLM5.0, and Cable-POP, and the S3 experiment in the simulation considering the adaptation
518    of $CO_2$, land use, N deposition, and climate from 1850 representing current environmental
519    conditions. We calculated the yearly mean Nup from 1984 to 2022 for each model, and the
520    average of all of them combined, to obtain a final yearly value. Then, we calculated the
521    difference between each model included in the TRENDY ensemble and our Nup estimations.
522    After, we averaged all the fNup values in a unique spatial explicit representation and
523    compared it with our estimations. We also calculated the latitudinal mean of the difference
524    to achieve a latitudinal profile and calculated the overall mean.
525

526 **Contributions**
527 H.V. and C.T. conceived the project; C.T. got the funding and supervised the work; H.V.,
528 C.M., A.K., J.C., and D.T. collected and compiled the data; H.V. curated and analyzed the
529 data, created the visuals and wrote the first draft; H.V., C.T., M.D.B., M.F.M., M.L., D.G.,
530 contributed with substantial ideas and feedback on the manuscript; all authors revised,
531 edited, and agreed on the final manuscript.
532
533 **Data availability statement**
534 The data gathered for this study, code and produced models are available at Zenodo
535 (Vallicrosa Pou, 2024).
536
537 **Competing interests**
538 The authors declare no competing interests
539

540 **Acknowledgments**
541 We acknowledge the members of the Terrer Lab for providing scientific consulting as well
542 as mental and emotional support during the investigation. We acknowledge the Pioneer
543 Center Land-CRAFT, Department of Agroecology, Aarhus University for making possible this
544 collaboration with D.G. J.C. was supported by the National Agency of Agricultural Research
545 of the Czech Republic (Project No. QK22020008) and the Ministry of Agriculture (CR),
546 institutional support MZE-RO0123, and he thanks FGMRI technician staff for help with field
547 and lab works. M.F.M was supported by the European Research Council project ERC-StG-
548 2022-101076740 STOIKOS and a Ramón y Cajal fellowship (RYC2021-031511-I) funded by
549 the Spanish Ministry of Science and Innovation, the NextGenerationEU program of the
550 European Union, the Spanish plan of recovery, transformation and resilience, and the
551 Spanish Research Agency.
552

553 **References**
554

555 Aber, J.D., Nadelhoffer, K.J., Steudler, P. & Melillo, J.M. (1989) Nitrogen saturation in northern forest
556 ecosystems. BioScience, 39, 378– 386.
557
558 Aber, J., and J. Melillo. 2001. Terrestrial ecosystems. Second edition. Harcourt Academic Press, San Diego,
559 California, USA.
560
561 Ackerman, D., Millet, D. B., & Chen, X. (2019). Global estimates of inorganic nitrogen deposition across
562 four decades. *Global Biogeochemical Cycles*, 33, 100– 107. https://doi.org/10.1029/2018GB005990
563
564 Arora, V. K., Katavouta, A., Williams, R. G., Jones, C. D., Brovkin, V., Friedlingstein, P., et al. (2020). Carbon-
565 concentration and carbon-climate feedbacks in CMIP6 models and their comparison to CMIP5 models.
566 Biogeosciences, 17(16), 4173–4222. https://doi.org/10.5194/ bg-17-4173-2020
567
568 Averill, C., Bhatnagar, J. M., Dietze, M. C., Pearse, W. D. & Kivlin, S. N. Global imprint of mycorrhizal fungi
569 on whole-plant nutrient economics. *Proc. Natl Acad. Sci. USA* 116, 23163–23168 (2019).
570

571 Bardgett, R., van der Putten, W. Belowground biodiversity and ecosystem functioning. *Nature* **515**, 505–
572 511 (2014). https://doi.org/10.1038/nature13855

574 Bartoń K (2023). _MuMIn: Multi-Model Inference_. R package version 1.47.5, <https://CRAN.R-
575 project.org/package=MuMIn>.

577 Battye, W., Aneja, V.P. and Schlesinger, W.H. (2017), Is nitrogen the next carbon? Earth's Future, 5: 894-
578 904. https://doi.org/10.1002/2017EF000592

580 Bauters, M., Verbeeck, H., Rütting, T., Barthel, M., Bazirake Mujinya, B., Bamba, F., Bodé, S., Boyemba, F.,
581 Bulonza, E., Carlsson, E., Eriksson, L., Makelele, I., Six, J., Cizungu Ntaboba, L., & Boeckx, P. (2019).
582 Contrasting nitrogen fluxes in African tropical forests of the Congo Basin. *Ecological Monographs*, *89*(1),
583 1–17. https://doi.org/10.1002/ecm.1342

585 Bauters, M., Janssens, I.A., Wasner, D. *et al.* Increasing calcium scarcity along Afrotropical forest
586 succession. *Nat Ecol Evol* 6, 1122–1131 (2022). https://doi.org/10.1038/s41559-022-01810-2

588 BERNTSON, G.M., RAJAKARUNA, N. and BAZZAZ, F.A. (1998), Growth and nitrogen uptake in an
589 experimental community of annuals exposed to elevated atmospheric CO2. Global Change Biology, 4:
590 607-626. https://doi.org/10.1046/j.1365-2486.1998.00171.x

592 Bobbink*, R. et al. Global assessment of nitrogen deposition effects on terrestrial plant diversity: a*
593 *synthesis. Ecol. Appl. 20, 30–59 (2010).*

595 Braghiere, R. K., Fisher, J. B., Allen, K., Brzostek, E., Shi, M., Yang, X., et al. (2022). Modeling global carbon
596 costs of plant nitrogen and phosphorus acquisition. *Journal of Advances in Modeling Earth Systems*, 14,
597 e2022MS003204. https://doi.org/10.1029/2022MS003204

599 Chen W, Koide RT, Eissenstat DM. Nutrient foraging by mycorrhizas: From species functional traits to
600 ecosystem processes. *Funct Ecol*. 2018; 32: 858–869. https://doi.org/10.1111/1365-2435.13041

602 Chen, T., and Guestrin, C. XGBoost: A scalable Tree Boosting System. arXiv:1603.02754v3

604 Chen T, He T, Benesty M, Khotilovich V, Tang Y, Cho H, Chen K, Mitchell R, Cano I, Zhou T, Li M, Xie J, Lin
605 M, Geng Y, Li Y, Yuan J (2023). _xgboost: Extreme Gradient Boosting_. R package version 1.7.5.1,
606 <https://CRAN.R-project.org/package=xgboost>.

608 Crowther TW, van den Hoogen J, Wan J, Mayes MA, Keiser AD, Mo L, et al. The global soil community and
609 its influence on biogeochemistry. Science. 2019;365:eaav0550.

611 Defourny, P. (2019): ESA Land Cover CCI project team; ESA Land Cover Climate Change Initiative
612 (Land_Cover_cci): Global Land Cover Maps, Version 2.0.7. Centre for Environmental Data Analysis, date
613 of citation. https://catalogue.ceda.ac.uk/uuid/b382ebe6679d44b8b0e68ea4ef4b701c

615 Delgado-Baquerizo M, Reich PB, Trivedi C, Eldridge DJ, Abades S, Alfaro FD, et al. Multiple elements of
616 soil biodiversity drive ecosystem functions across biomes. Nat Ecol Evol. 2020;4:210–20.

618 Du, E., Terrer, C., Pellegrini, A.F.A. et al. Global patterns of terrestrial nitrogen and phosphorus limitation.
619 Nat. Geosci. 13, 221–226 (2020). https://doi.org/10.1038/s41561-019-0530-4

621 Dybzinski, R., Segal, E., McCormack, M.L. et al. Calculating Nitrogen Uptake Rates in Forests: Which
622 Components Can Be Omitted, Simplified, or Taken from Trait Databases and Which Must Be Measured In
623 Situ?. Ecosystems 27, 739–763 (2024). https://doi.org/10.1007/s10021-024-00919-8

625 Elser JJ, Fagan WF, Kerkhoff AJ, Swensson NG, Enquist BJ. 2010. Biological stoichiometry of plant
626 production: metabolism, scaling and ecological response to global change. New Phytologist 186: 593–
627 608.

629 Etzold S, Ferretti M, Reinds GJ, Solberg S, Gessler A, Waldner P, Schaub M, Simpson D, Benham S, Hansen
630 K, Ingerslev M, Jonard M, Karlsson PE, Lindroos A-J, Marchetto A, Manninger M, Meesenburg H, Merilä P,
631 Nöjd P, Rautio P, Sanders TGM, Seidling W, Skudnik M, Thimonier A, Verstraeten A, Vesterdal L,
632 Vejpustková M, de Vries W (2020) Nitrogen deposition is the most important environmental driver of
633 growth of pure, even-aged and managed European forests. Forest Ecology and Management 458: 117762.
634 DOI: 10.1016/j.foreco.2019.117762

636 Fernández-Martínez, M., Vicca, S., Janssens, I. *et al.* Nutrient availability as the key regulator of global
637 forest carbon balance. *Nature Clim Change* 4, 471–476 (2014). https://doi.org/10.1038/nclimate2177

639 Fernández-Martínez, M., Sardans, J., Chevallier, F. *et al.* Global trends in carbon sinks and their
640 relationships with CO2 and temperature. *Nature Clim Change* 9, 73–79 (2019).
641 https://doi.org/10.1038/s41558-018-0367-7

643 Fick, S.E. and R.J. Hijmans, 2017. WorldClim 2: new 1km spatial resolution climate surfaces for global land
644 areas. International Journal of Climatology 37 (12): 4302-4315.

646 Finzi AC, Norby RJ, Calfapietra C, Gallet-Budynek A, Gielen B, Holmes WE, Hoosbeek MR, Iversen CM,
647 Jackson RB, Kubiske ME, Ledford J, Liberloo M, Oren R, Polle A, Pritchard S, Zak DR, Schlesinger WH,
648 Ceulemans R. 2007.Increases in nitrogen uptake rather than nitrogen-use efficiency support higher rates
649 of temperate forest productivity under elevated CO2. Proceedings of the National Academy of Sciences
650 104: 14014-14019.

652 Fleischer, K., Rammig, A., De Kauwe, M. G., Walker, A. P., Domingues, T. F., Fuchslueger, L., et al. (2019).
653 Amazon forest response to CO2 fertilization dependent on plant phosphorus acquisition. Nature
654 Geoscience, 12(9), 736–741. https://doi.org/10.1038/s41561-019-0404-9

656 Fowler D, Steadman CE, Stevenson D, Coyle M, Rees RM, Skiba UM, Sutton MA, Cape JN, Dore AJ, Vieno
657 M, Simpson D, et al. Effects of global change during the 21st century on the nitrogen cycle. Atmospheric
658 Chemistry and Physics. 2015; 15(24): 13849-13893. https://doi.org/10.5194/acp-15-13849-2015

660 Fox J, Weisberg S (2019). _An R Companion to Applied Regression_, Third edition. Sage, Thousand Oaks
661 CA. <https://socialsciences.mcmaster.ca/jfox/Books/Companion/>.

663 Franklin, O., Harrison, S.P., Dewar, R. *et al.* Organizing principles for vegetation dynamics. *Nat. Plants* 6,
664 444–453 (2020). https://doi.org/10.1038/s41477-020-0655-x

666 Giam, X. and Olden, J.D. (2016), Quantifying variable importance in a multimodel inference framework.
667 Methods Ecol Evol, 7: 388-397. https://doi.org/10.1111/2041-210X.12492

669 Gundersen, P., Emmett, B.A., Kjonaas, O.J., Koopmans, C.J. & Tietema, A. (1998) Impact of nitrogen
670 deposition on nitrogen cycling in forests: a synthesis of NITREX data. Forest Ecology and Management,
671 101, 37– 55.

Gurmesa, G.A., Wang, A., Li, S. *et al.* Retention of deposited ammonium and nitrate and its impact on the global forest carbon sink. *Nat Commun* 13, 880 (2022). https://doi.org/10.1038/s41467-022-28345-1

Hijmans R (2023). _raster: Geographic Data Analysis and Modeling_. R package version 3.6-20, https://CRAN.R-project.org/package=raster

Hungate, B.A., *et al.*, Nitrogen and Climate Change. *Science*302,1512-1513(2003). DOI:10.1126/science.1091390

Iversen C M, Bridgham S D and Kellogg L E 2010 Scaling plant nitrogen use and uptake efficiencies in response to nutrient addition in peatlands *Ecology* 91 693–707

Jackman, S (2020). pscl: Classes and Methods for R Developed in the Political Science Computational Laboratory. United States Studies Centre, University of Sydney. Sydney, New South Wales, Australia. R package version 1.5.5.1. URL https://github.com/atahk/pscl/

Kanakidou, M., Myriokefalitakis, S., Daskalakis, N., Fanourgakis, G., Nenes, A., Baker, A. R., Tsigaridis, K., & Mihalopoulos, N. (2016). Past, present, and future atmospheric nitrogen deposition. Journal of the Atmospheric Sciences, 73(5), 2039–2047. https://doi.org/10.1175/JAS-D-15-0278.1

Kuzyakov, Y. and Xu, X. (2013), Competition between roots and microorganisms for nitrogen: mechanisms and ecological relevance. New Phytol, 198: 656-669. https://doi.org/10.1111/nph.12235

Le Quéré, C. et al., Global Carbon Budget 2018, Earth Syst. Sci. Data, 10, 2141-2194, DOI: 10.5194/essd-10-2141-2018, 2018.

Lever, J., Krzywinski, M., & Altman, N. (2016). Model selection and overfitting. *Nature Methods*, **13**, 703–704.

McIntire E, Chubaty A (2023). _SpaDES.tools: Additional Tools for Developing Spatially Explicit Discrete Event Simulation (SpaDES) Models_. R package version 2.0.0, <https://CRAN.R-project.org/package=SpaDES.tools>.

Niu, S., Classen, A.T., Dukes, J.S., Kardol, P., Liu, L., Luo, Y., Rustad, L., Sun, J., Tang, J., Templer, P.H., Thomas, R.Q., Tian, D., Vicca, S., Wang, Y.-P., Xia, J. and Zaehle, S. (2016), Global patterns and substrate-based mechanisms of the terrestrial nitrogen cycle. Ecol Lett, 19: 697-709. https://doi.org/10.1111/ele.12591

Peng, Y, Chen, HYH, Yang, Y. Global pattern and drivers of nitrogen saturation threshold of grassland productivity. Funct Ecol. 2020; 34: 1979–1990. https://doi.org/10.1111/1365-2435.13622

Peng, Y., Prentice, I. C., Bloomfield, K. J., Campioli, M., Guo, Z., Sun, Y., Tian, Di, Wang, X., Vicca, S., & Stocker, B. D. (2023). Global terrestrial nitrogen uptake and nitrogen use efficiency. *Journal of Ecology*, 111, 2676–2693. https://doi.org/10.1111/1365-2745.14208

Penuelas, J, Janssens, IA, Ciais, P, Obersteiner, M, Sardans, J. Anthropogenic global shifts in biospheric N and P concentrations and ratios and their impacts on biodiversity, ecosystem productivity, food security, and human health. *Glob Change Biol*. 2020; 26: 1962– 1985. https://doi.org/10.1111/gcb.14981

Poggio, L., de Sousa, L. M., Batjes, N. H., Heuvelink, G. B. M., Kempen, B., Ribeiro, E., and Rossiter, D.: SoilGrids 2.0: producing soil information for the globe with quantified spatial uncertainty, SOIL, 7, 217–240, https://doi.org/10.5194/soil-7-217-2021, 2021.

726 Prentice, I. C., Liang, X., Medlyn, B. E., & Wang, Y.-P. (2015). Reliable, robust and realistic: The three R's
727 of next-generation land-surface modelling. Atmospheric Chemistry and Physics, 15(10), 5987–6005.
728 https://doi.org/10.5194/acp-15-5987-2015
729

730 Ruehr, S., Keenan, T.F., Williams, C. et al. Evidence and attribution of the enhanced land carbon sink. Nat
731 Rev Earth Environ 4, 518–534 (2023). https://doi.org/10.1038/s43017-023-00456-3
732

733 Shcherbak I, Millar N and Robertson G P 2014 Global metaanalysis of the nonlinear response of soil nitrous
734 oxide ($N_2O$) emissions to fertilizer nitrogen *Proc. Natl Acad. Sci. USA* 111 9199–204
735

736 Sinsabaugh, R., Carreiro, M. & Repert, D. Allocation of extracellular enzymatic activity in relation to litter
737 composition, N deposition, and mass loss. *Biogeochemistry* 60, 1–24 (2002).
738 https://doi.org/10.1023/A:1016541114786
739

740 Sinsabaugh, R.L., Lauber, C.L., Weintraub, M.N., Ahmed, B., Allison, S.D., Crenshaw, C., Contosta, A.R.,
741 Cusack, D., Frey, S., Gallo, M.E., Gartner, T.B., Hobbie, S.E., Holland, K., Keeler, B.L., Powers, J.S., Stursova,
742 M., Takacs-Vesbach, C., Waldrop, M.P., Wallenstein, M.D., Zak, D.R. and Zeglin, L.H. (2008), Stoichiometry
743 of soil enzyme activity at global scale. Ecology Letters, 11: 1252-1264. https://doi.org/10.1111/j.1461-
744 0248.2008.01245.x
745

746 Sitch, S., Friedlingstein, P., Gruber, N., Jones, S. D., Murray-Tortarolo, G., Ahlström, A., et al. (2015). Recent
747 trends and drivers of regional sources and sinks of carbon dioxide. Biogeosciences, 12(3), 653–679.
748 https://doi.org/10.5194/BG-12-653-2015
749

750 Soudzilovskaia, N.A., van Bodegom, P.M., Terrer, C. *et al.* Global mycorrhizal plant distribution linked to
751 terrestrial carbon stocks. *Nat Commun* **10**, 5077 (2019). https://doi.org/10.1038/s41467-019-13019-2
752

753 Soudzilovskaia, N.A., Vaessen, S., Barcelo, M., He, J., Rahimlou, S., Abarenkov, K., Brundrett, M.C., Gomes,
754 S.I.F., Merckx, V. and Tedersoo, L. (2020), FungalRoot: global online database of plant mycorrhizal
755 associations. New Phytol, 227: 955-966. https://doi.org/10.1111/nph.16569
756

757 Stevens C J, Lind E M, Hautier Y and Harpole W S 2015 Anthropogenic nitrogen deposition predicts local
758 grassland primary production worldwide *Ecology* 96 1459–65
759

760 Stocker BD, Prentice IC, Cornell SE, Davies-Barnard T, Finzi AC, Franklin O, Janssens I, Larmola T, Manzoni
761 S, Näsholm T, Raven JA, et al. Terrestrial nitrogen cycling in Earth system models revisited. New
762 Phytologist. 2016; 210(4): 1165-1168. https://doi.org/10.1111/nph.13997
763

764 Sutton, M.A.; Fowler, D. 1993 Estimating the relative contribution of SOx, NOy and NHx inputs to effects
765 of atmospheric deposition Critical loads: concept and applications. Grange-over-Sands Workshop
766

767 Terrer, C., Jackson, R. B., Prentice, I. C., Keenan, T. F., Kaiser, C., Vicca, S., et al. (2019). Nitrogen and
768 phosphorus constrain the CO2 fertilization of global plant biomass. Nature Climate Change, 9(9), 684–
769 689. https://doi.org/10.1038/s41558-019-0545-2
770

771 Tian, D., Wang H.,, Sun, J., and Niu, S. Global evidence on nitrogen saturation of terrestrial ecosystem net
772 primary productivity. 2016. Environmental Research Letters, Volume 11, Number 2
773

774 Tian, D., Kattge, J., Chen, Y., Han, W., Luo, Y., He, J., Hu, H., Tang, Z., Ma, S., Yan, Z., Lin, Q., Schmid, B.,
775 Fang, J. 2019. A global database of paired leaf nitrogen and phosphorus concentrations of terrestrial
776 plants. Ecology 100(9): e02812.
777

778 Vallicrosa, H., J. Sardans, J. Maspons, and J. Peñuelas. 2022. "Global distribution and drivers of forest
779 biome foliar nitrogen to phosphorus ratios (N:P)." Global Ecology and Biogeography 31: 861–71.
780
781 Vallicrosa Pou, H. (2024). Global plant nitrogen uptake and nitrogen use efficiency. Zenodo.
782 https://doi.org/10.5281/zenodo.13332734
783
784 Vicca, S., Stocker, B. D., Reed, S., Wieder, W. R., Bahn, M., Fay, P. A., Janssens, I. A., Lambers, H., Peñuelas,
785 J., Piao, S., Rebel, K. T., Sardans, J., Sigurdsson, B. D., Sundert, K. V., Wang, Y. P., Zaehle, S., and Ciais, P.:
786 Using research networks to create the comprehensive datasets needed to assess nutrient availability as
787 a key determinant of terrestrial carbon cycling, Environ. Res. Lett., 13,
788 125006,https://doi.org/10.1088/1748-9326/aaeae7, 2018.
789
790 Walker, T. W., and J. K. Syers. 1976. "Fate of Phosphorus during Pedogenesis." Geoderma 15: 1–19.
791 Soudzilovskaia, N.A., van Bodegom, P.M., Terrer, C. *et al.* Global mycorrhizal plant distribution linked to
792 terrestrial carbon stocks. *Nat Commun* 10, 5077 (2019). https://doi.org/10.1038/s41467-019-13019-2
793
794 Walker, A.P., De Kauwe, M.G., Bastos, A., Belmecheri, S., Georgiou, K., Keeling, R.F., McMahon, S.M.,
795 Medlyn, B.E., Moore, D.J.P., Norby, R.J., Zaehle, S., Anderson-Teixeira, K.J., Battipaglia, G., Brienen, R.J.W.,
796 Cabugao, K.G., Cailleret, M., Campbell, E., Canadell, J.G., Ciais, P., Craig, M.E., Ellsworth, D.S., Farquhar,
797 G.D., Fatichi, S., Fisher, J.B., Frank, D.C., Graven, H., Gu, L., Haverd, V., Heilman, K., Heimann, M., Hungate,
798 B.A., Iversen, C.M., Joos, F., Jiang, M., Keenan, T.F., Knauer, J., Körner, C., Leshyk, V.O., Leuzinger, S., Liu,
799 Y., MacBean, N., Malhi, Y., McVicar, T.R., Penuelas, J., Pongratz, J., Powell, A.S., Riutta, T., Sabot, M.E.B.,
800 Schleucher, J., Sitch, S., Smith, W.K., Sulman, B., Taylor, B., Terrer, C., Torn, M.S., Treseder, K.K., Trugman,
801 A.T., Trumbore, S.E., van Mantgem, P.J., Voelker, S.L., Whelan, M.E. and Zuidema, P.A. (2021), Integrating
802 the evidence for a terrestrial carbon sink caused by increasing atmospheric CO2. New Phytol, 229: 2413-
803 2445. https://doi.org/10.1111/nph.16866
804
805 Wall, D. H., Nielsen, U. N. & Six, J. Soil biodiversity and human health. *Nature* **528**, 69–76 (2015).
806
807 Wang R, Goll D, Balkanski Y, Hauglustaine D, Boucher O, Ciais P, Janssens I, Pe~ nuelas J, Guenet B, Sardans
808 J et al. 2017. Global forest carbon uptake due to nitrogen and phosphorus deposition from 1850–2100.
809 Global Change Biology 23: 4854–4872.
810
811 Wang, X., Zhao, X. (Eds.), 2022. Protocol for Field Investigation and Literature Data Compilation of Carbon
812 Storage in Terrestrial Ecosystems. Science Press, Beijing.
813
814 Wickham, H. ggplot2: Elegant Graphics for Data Analysis. Springer-Verlag New York, 2016.
815
816 Wickham H, Henry L (2023). _purrr: Functional Programming Tools_. R package version 1.0.2,
817 <https://CRAN.R-project.org/package=purrr>.
818
819 WU, Z., DIJKSTRA, P., KOCH, G.W., PEÑUELAS, J. and HUNGATE, B.A. (2011), Responses of terrestrial
820 ecosystems to temperature and precipitation change: a meta-analysis of experimental manipulation.
821 Global Change Biology, 17: 927-942. https://doi.org/10.1111/j.1365-2486.2010.02302.x
822
823 Xu, X., Thornton, P.E. and Post, W.M. (2013), Global soil microbial biomass C, N and P. Global Ecology and
824 Biogeography, 22: 737-749. https://doi.org/10.1111/geb.12029
825
826 Yang, J. and Tian, H. (2022): ISIMIP3a N-deposition input data (v1.2). ISIMIP Repository.
827 https://doi.org/10.48364/ISIMIP.759077.2
828

829 Zaehle S, Medlyn BE, De Kauwe MG, Walker AP, Dietze MC, Hickler T, Luo Y, Wang YP, El-Masri B, Thornton
830 P, Jain A, et al. Evaluation of 11 terrestrial carbon-nitrogen cycle models against observations from two
831 temperate Free-Air $CO_2$ Enrichment studies. New Phytologist. 2014; 202(3): 803-822.
832 https://doi.org/10.1111/nph.12697
833
834 Zhou G, Terrer C, Huang A, Hungate BA, van Gestel N, Zhou X, van Groenigen KJ. Nitrogen and water
835 availability control plant carbon storage with warming. Sci Total Environ. 2022 Dec 10;851(Pt 1):158243.
836 doi: 10.1016/j.scitotenv.2022.158243. Epub 2022 Aug 23. PMID: 36007637.